Article

Influence of the C Terminus of Wiskott-Aldrich Syndrome Protein (WASp) and the Arp2/3 Complex on Actin Polymerization

Henry N. Higgs, Laurent Blanchoin, and Thomas D. Pollard

Biochemistry, **1999**, 38 (46), 15212-15222• DOI: 10.1021/bi991843+ • Publication Date (Web): 29 October 1999

Influence of the C Terminus of Wiskott-Aldrich Syndrome Protein (WASp) and the Arp2/3 Complex on Actin Polymerization†

Henry N. Higgs, Laurent Blanchoin, and Thomas D. Pollard*

Structural Biology Laboratory, The Salk Institute for Biological Studies, 10010 North Torrey Pines Road, La Jolla, California 92037

Received August 6, 1999; Revised Manuscript Received September 22, 1999

ABSTRACT: The 70 C-terminal amino acids of Wiskott-Aldrich syndrome protein (WASp WA) activate the actin nucleation activity of the Arp2/3 complex. WASp WA binds both the Arp2/3 complex and actin monomers, but the mechanism by which it activates the Arp2/3 complex is not known. We characterized the effect of WASp WA on actin polymerization in the absence and presence of the human Arp2/3 complex. WASp WA binds actin monomers with an apparent K_d of 0.4 μM, inhibiting spontaneous nucleation and subunit addition to pointed ends, but not addition to barbed ends. A peptide containing only the WASp homology 2 motif behaves similarly but with a 10-fold lower affinity. In contrast to previously published results, neither WASp WA nor a similar region of the protein Scar1 significantly depolymerizes actin filaments under a variety of conditions. WASp WA and the Arp2/3 complex nucleate actin filaments, and the rate of this nucleation is a function of the concentrations of both WASp WA and the Arp2/3 complex. With excess WASp WA and <10 nM Arp2/3 complex, there is a 1:1 correspondence between the Arp2/3 complex and the concentration of filaments produced, but the filament concentration plateaus at an Arp2/3 complex concentration far below the cellular concentration determined to be 9.7 μM in human neutrophils. Preformed filaments increase the rate of nucleation by WASp WA and the Arp2/3 complex but not the number of filaments that are generated. We propose that filament side binding by the Arp2/3 complex enhances its activation by WASp WA.

Many cells require actin polymerization for cell motility. As cells move, new filaments grow from their barbed ends in a cross-linked meshwork at the leading edge (reviewed in ref *1*). New filaments are created by nucleation of monomeric actin (*2*, *3*). Nucleation is the rate-limiting step of actin polymerization, as the dimer and trimer intermediates in this process are extremely unstable (reviewed in ref *4*). Elucidation of the mechanisms by which cells overcome this unfavorable nucleation step to polymerize actin rapidly upon stimulation has been a long-standing goal.

Recent studies suggest that the Arp2/3 complex is an important cellular nucleating factor. The Arp2/3 complex, present in all eukaryotes examined, consists of seven polypeptides, including two actin-related proteins, Arp2 and Arp3 (reviewed in ref *5*). Molecular modeling studies predicted that Arp2 and Arp3 might form a stable nucleus for barbed end elongation, thereby overcoming the slow nucleation step (*6*). The Arp2/3 complex concentrates to areas of actin polymerization and translocates to areas of new actin polymerization upon stimulation (*7*, *8*). Cdc42, a Rho family GTPase that regulates actin polymerization in many cell processes, requires Arp2/3 complex to stimulate actin polymerization in cell extracts (*9*, *10*).

Actin polymerization assays in vitro show that the Arp2/3 complex alone is a weak nucleator (*11*). Several proteins greatly stimulate its nucleation activity. One protein is ActA, the sole protein required for actin-based motility of the bacterium, *Listeria monocytogenes*, in the cytoplasm of eukaryotic cells (*12*). Members of the WASp/Scar protein family also stimulate nucleation by Arp2/3 complex (reviewed in ref *13*). This family consists of the mammalian members: WASp (Wiskott-Aldrich syndrome protein), N-WASP, and three isoforms of Scar (Scar1, -2, and -3), as well as Bee1 (Las17p) in *Saccharomyces cerevisiae* and Scar (supressor of cAMP receptor disruption) in *Dictyostelium discoidium*. Optimal stimulation of nucleation requires the C-terminal regions of WASp/Scar proteins (WA). The WA region, including a WASp homology 2 motif (WH2) and an acidic C terminus, can bind both actin monomers and the Arp2/3 complex. Many aspects of this activation are not understood, including the role of actin monomer binding by WASp/Scar proteins.

In addition to nucleating actin, the Arp2/3 complex also cross-links the pointed end of one filament to the side of another to create a "Y branch" in vitro (*11*). Actin in the extreme leading edge of motile cells is also cross-linked into Y branches, and the Arp2/3 complex localizes to the junctions of these cross-links (*14*−*16*). The dual abilities of the Arp2/3 complex to nucleate and cross-link actin filaments led to the dendritic nucleation model, whereby the complex uses these two activities to create a filament meshwork at the leading edge (*11*).

† This work was supported by NIH Research Grant GM-26338 to T.D.P. and an NIH National Research Service Award to H.N.H.

* To whom correspondence should be addressed: The Salk Institute for Biological Studies, 10010 N. Torrey Pines Rd., La Jolla, CA 92037. Telephone: (619) 453-4100, ext, 1261. Fax: (619) 452-3683. E-mail: pollard@salk.edu.

10.1021/bi991843+ CCC: $18.00
Published on Web 10/29/1999

The dendritic nucleation model has been supported by the finding that actin filaments enhance nucleation by the Arp2/3 complex and WA in vitro (*17*). Without filaments, the initial lag in actin polymerization nucleated by the Arp2/3 complex and Scar1WA is appreciable. Sub-micromolar concentrations of polymerized actin virtually eliminate this lag. Since WASp/Scar WA regions do not appear to bind filaments (*18*), this suggests that Arp2/3 complex binding to the side of a filament also stimulates nucleation by the complex. This finding suggests that cross-linking and nucleation by the Arp2/3 complex might be intimately linked, facilitating formation of a cross-linked actin meshwork at the leading edge.

In this paper, we use human WASp WA and the human leukocyte Arp2/3 complex to address several questions. How does WASp WA bind actin monomers? Is filament side binding by the Arp2/3 complex essential for nucleation, or does side binding stimulate nucleation? What other conditions (pH and the state of actin monomers) affect nucleation by the Arp2/3 complex and WA? Finally, what is the concentration of the Arp2/3 complex in leukocytes, and do our kinetic results make sense in terms of this concentration?

EXPERIMENTAL PROCEDURES

Preparation of WASp WA and Scar1 WA. DNA encoding human WASp amino acids 429−503 or human Scar1 amino acids 443−559 was cloned into pGEX-2T (Amersham/Pharmacia) and expressed and purified as described previously (*17*).

Quantitative Immunoblotting. Polymorphonuclear leukocytes (PMN) were purified from human blood leukocytes (obtained as described below) by layering 5 mL of leukocytes onto 7 mL of Ficoll-Hypaque (Amersham/Pharmacia) in a 50 mL conical tube (Falcon) and centrifuging in a swinging bucket rotor at 500*g* at R_{max} for 15 min at 4 °C. The supernatant was removed, and the pellet was washed once in 25 mL of KRH and then resuspended to a density of 4×10^8/mL in KRH. This cell suspension consisted of greater than 90% PMN. After detergent extraction (described below), 20 μL aliquots of uncentrifuged homogenate were flash-frozen in liquid nitrogen and stored at −80 °C. The total protein concentration was determined by the Bradford assay (Bio-Rad). 5× SDS−PAGE sample buffer [150 mM Tris-HCl (pH 6.8), 25% glycerol, 10% SDS, 12.5% β-mercaptoethanol, 2.5 mM EDTA, and 0.001% bromophenol blue] was brought to boiling and added to the frozen homogenate to a protein concentration of 2 μg/mL (cell density of 4.4×10^6 cells/mL), and further boiled for 5 min. This stock was diluted in 1× SDS−PAGE sample buffer with or without varying concentrations of 6His-p34 (concentration of 6His-p34 determined by densitometry of Coomassie-stained SDS−PAGE using the *Acanthamoeba* Arp2/3 complex and actin as standards). SDS−PAGE was conducted on 15 cm gels (Hoeffer), and the proteins were transferred onto a PVDF membrane overnight at 20 V/gel in 10 mM CAPS (pH 11.0) and 10% methanol. The membrane was blocked in TBST [50 mM Tris-HCl (pH 7.5), 100 mM NaCl, and 0.1% Tween 20] containing 3% BSA for 4 h at 20 °C, and then incubated for 16 h in TBST and 0.3% BSA containing affinity-purified anti-p34 diluted 1:2000 at 4 °C. After extensive washing in TBST, the membrane was treated with a 1:5000 dilution of horseradish peroxidase-congugated goat anti-rabbit IgG (Babco) in TBST for 90 min. The blot was again washed extensively in TBST, and immunoreactive bands were revealed by ECL (Amersham/Pharmacia). Figure 2 is a 3 s exposure of one such blot. Band intensity was quantified by densitometry of a 1 s exposure of the same blot. The integrated band density of 6His-p34 varied linearly between 5 and 20 ng (not shown). The cytoplasmic concentration was determined on the basis of a cytoplasmic volume of 1.8×10^{-13} L per PMN, as calculated by morphometry in which the volumes of granules and the nucleus were subtracted from the total cell volume (*19*).

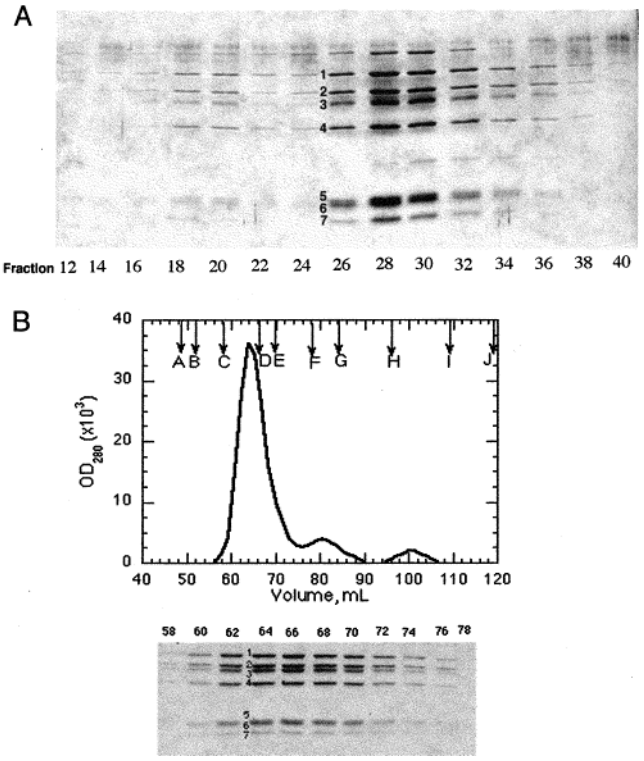

FIGURE 1: Purification of the Arp2/3 complex from human leukocytes. (A) Coomassie-stained SDS−PAGE of MonoS fractions. (B) Superdex 200 elution profile of Arp2/3 complex MS2 and Coomassie-stained SDS−PAGE of Superdex 200 fractions. MS1 migrated similarly (not shown). Standards eluted on Superdex 200 as follows: A being blue dextran 2000, B thyroglobulin (669 kDa), C ferritin (440 kDa), D catalase (232 kDa), E aldolase (158 kDa), F BSA (67 kDa), G ovalbumin (43 kDa), H chymotrypsinogen (25 kDa), I RNase A (13 kDa), and J vitamin B_{12} (1.4 kDa). Subunits are labeled as follows: 1 being Arp3, 2 Arp2, 3 p40, 4 p34, 5 p21, 6 p20, and 7 p16.

Purification of the Arp2/3 Complex. Table 1 summarizes the steps and yields. Human peripheral leukocytes were prepared from 6 units of blood drawn into ACD (29.4 g/L citric acid monohydrate, 58.8 g/L sodium citrate, and 39.6 g/L dextrose). Each unit was mixed with 0.1 volume of 10% Dextran T500 (Amersham/Pharmacia) in 0.9% NaCl, poured into a 1000 mL separatory funnel, and incubated at 25 °C for 30 min. Red cells were drained off, and the upper phases were centrifuged at 500*g* for 15 min at 25 °C. The remaining red cells were lysed by resuspending each pellet in 25 mL of iced LB (8.3 g/L ammonium chloride, 1 g/L sodium bicarbonate, and 0.038 g/L disodium EDTA, with the pH not adjusted), incubated on ice for 5 min, and centrifuged for 5 min at 200*g*. The pellets were washed in 25 mL of

Table 1: Arp2/3 Complex Purification from Human Leukocytes

fraction	total volume (mL)	total protein[a] (mg)	Arp2/3 complex (mg)	fold enrichment[d]
homogenate	36	350	4.1[b]	1
LSS	38	176	3.5[b]	1.7
Q FT	45	81	3.1[b]	3.3
SourceQ eluate	40	7.2	3.0[c]	36
MonoS peak 1	7	0.5	0.3[c]	51
MonoS peak 2	10	2.9	2.6[c]	77
S200 (MS1)	6	0.25	0.25[c]	85
S200 (MS2)	6	2.4	2.4[c]	85

[a] Total protein determined by the Bradford assay. [b] Arp2/3 complex concentration determined by quantitative immunoblotting using the anti-p34 antibody. [c] Arp2/3 complex concentration determined by scanning of Coomassie-stained SDS−PAGE using the *Acanthamoeba* Arp2/3 complex as a standard. [d] Calculated by dividing the number of milligrams of Arp2/3 complex in a given purification step by the number of milligrams in the homogenate.

0.9% NaCl per pellet. The six pellets were combined in 50 mL of 0.9% NaCl; 3 mM diisopropyl fluorophosphate was added, and the cells were incubated on ice for 15 min. The cells were pelleted and resuspended to a density of 4×10^8 cells/mL in KRH [118 mM NaCl, 9.7 mM KCl, 25 mM HEPES (pH 7.4), 1.2 mM KH_2PO_4, and 1.2 mM $MgSO_4$]. This suspension, which consisted of 70% polymorphonuclear cells and 30% mononuclear cells, was incubated at 37 °C for 10 min, and then stimulated with 0.001 volume of 1 mM fMLP in DMSO for 10 s. An equal volume of iced extraction buffer [40 mM Tris-HCl (pH 8.0), 5 mM EDTA, 1 mM DTT, 0.5% Thesit (Roche Biochemicals), 20 μg/mL leupeptin, and 10 μg/mL pepstatin A] was added, mixed by inversion for 1 min at 4 °C, and centrifuged at 20000*g* for 5 min. The conductivity of the supernatant (LSS) was adjusted to that of QA [10 mM Tris-HCl (pH 8.0), 100 mM NaCl, 1 mM EGTA, 1 mM $MgCl_2$, and 1 mM DTT] with 5 M NaCl and loaded by gravity flow onto a 5 mL column of Q Fast Flow (Amersham/Pharmacia) equilibrated in QA. The column was washed with 5 mL of QA, and the flow through plus wash was dialyzed against several changes of 1 mM Tris-HCl (pH 8.0), 0.1 mM EGTA, 0.1 mM $MgCl_2$, and 1 mM DTT until the conductivity was equal to that of QB [10 mM Tris-HCl (pH 8.0), 1 mM EGTA, 1 mM $MgCl_2$, and 1 mM DTT]. The dialysate was loaded onto 8 mL of Source Q15 packed in a 10/10 column (Amersham/Pharmacia) equilibrated in QB. After washing the column with QB until the 280 nm absorbance returned to baseline, bound proteins were eluted with an 80 mL linear gradient to QA. Fractions containing the Arp2/3 complex were detected by actin nucleation assays in the presence of WASp WA. These fractions were pooled and diluted 1:1 into SA [20 mM PIPES (pH 6.8), 50 mM NaCl, 1 mM EGTA, 1 mM $MgCl_2$, and 1 mM DTT] and loaded onto a MonoS 10/10 column (Amersham/Pharmacia) equilibrated in SA. After washing the column with SA until the 280 nm absorbance returned to baseline, bound proteins were eluted with a 160 mL linear gradient to SB (SA but with 250 mM NaCl). Two peaks of the Arp2/3 complex eluted (Figure 1A), centered at 105 (MS1) and 120 mM NaCl (MS2). Each peak was pooled separately, concentrated in a Centricon50 apparatus (Amicon), and loaded onto 125 mL of Superdex 200 packed in a 16/60 column (Amersham/Pharmacia) and equilibrated with SB. The Arp2/3 complex in each peak eluted with a Stoke's radius equivalent to that of a 240 kDa globular particle. No other protein bands could be visualized by Coomassie staining (Figure 1B). The purified Arp2/3 complex was dialyzed against 2 mM Tris-HCl (pH 8.0), 0.1 mM EGTA, 0.1 mM $MgCl_2$, 1 mM DTT, and 75% glycerol and stored at −20 °C. Concentrations of the Arp2/3 complex from SourceQ 15, MonoS, and Superdex 200 columns were measured by Coomassie staining of SDS−PAGE using the *Acanthamoeba* Arp2/3 complex as a standard. Three concentrations of the PMN Arp2/3 complex and four concentrations of the *Acanthamoeba* Arp2/3 complex were used. The gels were scanned, and the integrated densities of the combined Arp2/Arp3 bands, the p34 band, and the combined p21/p20 bands were measured separately in NIH Image. The concentration of the PMN Arp2/3 complex was based on an average of these three separate measurements against curves for the *Acanthamoeba* Arp2/3 complex. The concentrations determined from the Arp2/Arp3, p43, and p21/p20 bands never differed by more than 5%. Although WASp WA activated both MS1 and MS2 comparably (not shown), MS2 was used for all subsequent characterization of activation by WA.

Other Proteins. Actin was purified from rabbit skeletal muscle (*20*). Monomers were purified by gel filtration on Sephacryl S-300 in G-buffer [2 mM Tris (pH 8.0), 0.2 mM ATP, 0.1 mM $CaCl_2$, and 0.5 mM DTT]. Actin was labeled (*21*) with pyrenyliodoacetamide (Molecular Probes, Eugene, OR), and the extent of labeling was determined using extinction coefficients of 22 000 M^{-1} cm^{-1} at 344 nm for bound pyrene and 26 600 M^{-1} cm^{-1} at 290 nm (*22*) for actin after correction for pyrene (*23*). Actin monomers were converted to ϵ-ADP or to ADP following the method described previously (*24*). ADP−P_i filaments were prepared by addition of 5 mM sodium phosphate (pH 7.0) to 5 μM actin previously polymerized for 1 h in 1× KMEI (*25*). ADP−BeF filaments were prepared by polymerizing 20 μM MgATP actin in 0.1 M KCl, 2 mM $MgCl_2$, 15 mM NaF, and 150 μM $BeCl_2$ at room temperature for 4 h (*26*). Recombinant human gelsolin was expressed in bacteria from the PET 23 vector (a generous gift from H. Yin) and purified following previously published methods (*27*). Spectrin−actin seeds were prepared from human erythrocytes (*28*). The recombinant p35 subunit of the human Arp2/3 complex with an N-terminal six-histidine tag (PET15b vector, Novagen) was expressed in *Escherichia coli* BL21(DE3), and purified from the high-speed pellet of the bacterial lysate by solubilization in 8 M urea and Ni−NTA chromatography (Qiagen) according to the manufacturer's instructions. This material was used to raise polyclonal antiserum in New Zealand white rabbits. Anti-p35 antibodies were purified by using their affinity for recombinant p35 as previously described (*29*). The WASp WH2 peptide (residues 432−456) was synthesized on an Applied Biosystems 432A peptide synthesizer and deprotected according to the manufacturer's instructions. The pure peptide gave a mass of 2666 Da as determined by MALDI (Salk Institute Mass Spectrometry Facility).

Gelsolin−Actin Seeds. Unlabeled actin in G-buffer was polymerized at a concentration of 8 μM by the addition of 0.1 volume of 10× KMT [500 mM KCl, 10 mM $MgCl_2$, and 100 mM Tris-HCl (pH 8.0)] for 1 h at 25 °C, then diluted 1:1 with 175 nM freshly purified gelsolin and 0.5 mM $CaCl_2$ in G-buffer with 0.1 volume of 10× KMT, and incubated

for 30 min at 25 °C. EGTA was added to a final concentration of 1 mM. The concentration of pointed ends was determined by measuring the elongation rate of pyrene−actin from these seeds using the equation [pointed ends] = elongation rate/(k_+[actin]), where $k_+ = 1.3\ \mu M^{-1}\ s^{-1}$ (*24*).

Effect of WASp WA on Nucleotide Exchange from Actin. The dissociation of Mg-ϵ-ADP from actin monomers was measured by the decrease in fluorescence with excitation at 360 nm and emission at 410 nm. A Hi-tech SFA-II rapid mixer enabled mixing of 600 μM ATP from one syringe with 2.8 μM ϵ-ADP actin in the absence or presence of 6 μM WASp WA in G-buffer-Mg (G-buffer with 1 mM EGTA and 0.1 mM $MgCl_2$).

Actin Polymerization by Fluorescence Spectroscopy. Pyrene-labeled and unlabeled actin monomers were mixed to obtain the desired ratio of pyrene−actin to unlabeled actin (5% pyrene−actin unless otherwise indicated), and diluted to 20 μM total actin in G-buffer. An aliquot of this stock was converted to Mg−actin by adding 0.1 volume of 10 mM EGTA and 1 mM $MgCl_2$ and incubating at 25 °C for 2 min in a 1.5 mL Eppendorf tube. This mix was diluted with G-buffer-Mg, and aliquots of the other proteins in the assay (in G-buffer-Mg) were placed in separate drops on the side of the tube. The reaction was started by adding 10× KMEI [500 mM KCl, 10 mM $MgCl_2$, 10 mM EGTA, and 100 mM imidazole (pH 7.0)] to the actin to a final concentration of 1×, and the separate drops of other proteins were quickly mixed into the actin; the final mix was placed into the cuvette, and the fluorescence reading was started. The delay between addition of 10× KMEI and the other proteins to the actin was <5 s, and the delay between starting the reaction and starting the fluorimeter was 12−17 s. Pyrene fluorescence data (excitation at 365 nm and emission at 407 nm) were collected on a PTI Alphascan spectrofluorimeter (Photon Technology International, Santa Clara, CA) at a rate of 1 point/s.

Calculation of Polymerization Parameters. We calculated the concentration of barbed ends from elongation rates using the equation [barbed ends] = elongation rate/(k_+[actin monomers]), where $k_+ = 11.6\ \mu M^{-1}\ s^{-1}$ at pH 7.0 (*24*). This method, using the elongation rate at the point where 80% of the monomers were polymerized in a spontaneous assembly reaction, gave the same concentration of ends as the initial rate of elongation when fresh monomers where added at the completion of spontaneous polymerization. We calculated k_+ at other pH values to be 18 (pH 6.5 imidazole), 15.9 (pH 6.75 imidazole or MOPS), 10.9 (pH 7.25 imidazole or MOPS), 8.7 (pH 7.5 MOPS or Tris), 7.1 (pH 7.75 MOPS or Tris), and 5.8 $\mu M^{-1}\ s^{-1}$ (pH 8.0 Tris) from elongation rates in the presence of actin monomers and a known concentration of actin filaments (buffer composition was 10 mM pH buffer, 1 mM EGTA, 1 mM $MgCl_2$, and 50 mM KCl). We defined polymerization lag as the time necessary for polymerization of 10% of the actin monomers (as judged by pyrene fluorescence) and nucleation rate as the inverse of the polymerization lag, with the full understanding that nucleation is more complex than this simple definition and that nucleation is occurring throughout this period (*4*). To calculate the apparent equilibrium constant of WA for actin monomers from the rate of inhibition of pointed end elongation, we used the equation

$$\Delta V_i = V_{ia} + (V_{ip} - V_{ia})[K_d + [A] + [WA] - \sqrt{(K_d + [A] + [WA])^2 - 4[A][WA]/2}]$$

where ΔV_i is the change in the initial rate of elongation, V_{ia} the initial elongation rate in the absense of WA, V_{ip} the initial elongation rate in the presence of WA, [A] the concentration of actin monomers, and [WA] the concentration of WA.

Pelleting Assays. Unlabeled actin was polymerized at a concentration of 5 μM in G-buffer with 1× KMEI for 1 h at 25 °C. Polymerized actin was diluted to a concentration of 4 μM in G-buffer and 1× KMEI containing the other proteins in the assay, and incubated for 30 min at 25 °C. The mixture was centrifuged at 80 000 rpm for 20 min in a TLA-100 rotor (Beckman) at 25 °C. The supernatant was removed, the surface of the pellet washed with 1× KMEI, and the pellet resuspended in 30 mM Tris-HCl (pH 6.8), 5% glycerol, 2.5% BME, 0.5 mM EDTA, and 6 M urea. Pellets and supernatants were analyzed by SDS−PAGE.

RESULTS

Purification of the Arp2/3 Complex. We developed a method for purifying the Arp2/3 complex from human leukocytes that features three advances over existing methods of mammalian Arp2/3 complex purification (*7*, *9*, *30*). First, the procedure is completed within 12 h of drawing the blood and within 8 h of lysing the leukocytes, minimizing the opportunity for protein modification or proteolysis after lysis. Second, the yield is about 5-fold higher than with other procedures. This high yield is in part due to the efficiency of the purification steps (67% recovery from the cell homogenate) and in part to the abundance of the Arp2/3 complex in leukocytes. The Arp2/3 complex represents 1.2% of the total cellular protein in neutrophils, or 9.7 ± 1.2 μM in the neutrophil cytoplasm (Figure 2). Approximately 70% of the cells in the total leukocyte preparation are neutrophils. Third, we identify two chromatographically distinct populations of the Arp2/3 complex by cation exchange chromatography, MS1 and MS2. While two populations of the Arp2/3 complex have been identified in *Acanthamoeba* (*31*), there are no reports of such heterogeneity in mammals. MS1 and MS2 exhibited comparable nucleation activities in the presence of WASp WA (not shown).

WASp WA Binds Actin Monomers and Inhibits Pointed End Elongation. All WASp/Scar members tested in previous studies bound actin monomers (*18*, *32*−*34*), but the experiments were not quantitative and did not reveal the effect of binding on actin polymerization. We determined the effect of WASp WA alone on actin polymerization before studying its effect on polymerization mediated by the Arp2/3 complex. WA inhibits spontaneous polymerization of actin monomers in a concentration-dependent manner (Figure 3A). However, at steady state even high concentrations of WA do not alter the polymer concentration as judged by pyrene fluorescence (not shown). Therefore, WA does not sequester actin monomers or cap the fast-growing barbed end of filaments, either of which changes the steady state polymer concentration. Instead, WA may inhibit nucleation or elongation. Excess WA inhibits slightly the rate of elongation from prepolymerized actin seeds by ATP−actin monomers (not shown). This is consistent with an effect on pointed end but

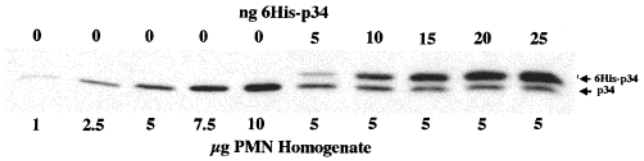

FIGURE 2: Determination of the p34 concentration in PMN by quantitative immunoblotting. A 10-fold concentration range of PMN homogenate was blotted, as well as a concentration curve of 6His-p34 in 5 μg of PMN homogenate as an internal control. The integrated density of p34 immunostaining was linear between 2.5 and 10 μg of homogenate, and between 5 and 20 ng of 6His-p34.

not barbed end elongation, since elongation from the pointed end is 10-fold slower than it is from the barbed end (*24*). We further tested elongation using filaments capped at the barbed end with gelsolin. Excess WA inhibits pointed end elongation (Figure 3B). Because the WA concentration dependence of this inhibition depends on the concentration of actin monomer but not on the concentration of gelsolin−actin seeds (not shown), we conclude that the inhibition is due to interaction of WA and actin monomers. From the dependence of this inhibition on WA concentration (Figure 3C), the apparent K_d of WA for actin monomers is 0.4 μM. Elongation from spectrin−actin seeds was 20% inhibited by saturating WA (Figure 3C), which might reflect a slightly decreased rate of barbed end elongation.

The effect of WA on pointed end elongation was similar to that of profilin (*35*, *36*). We therefore tested whether WA might also be like profilin in catalyzing nucleotide exchange on actin. However, the rate of ϵ-ATP exchange on actin is the same in the presence and absence of excess WA (not shown).

The WH2 motif of WASp/Scar proteins contributes to actin monomer binding (*33*). To test whether this motif is sufficient to bind monomers, we synthesized and tested a peptide of WH2. Like WA, WH2 inhibits nucleation and pointed end elongation (panels A and B of Figure 3). The K_d of WH2 for actin monomers estimated from its inhibition of pointed end elongation is 5 μM, about 10-fold higher than for WA.

While previous studies agree that the C-termini of WASp/Scar proteins do not bind tightly to actin filaments (*18*, *32*−*34*), these studies differ on the issue of whether these proteins depolymerize actin filaments. The fact that, in our experiments, actin eventually polymerizes fully even in excess WA shows that WA does not sequester actin monomers. However, studies where depolymerization was observed (*32*−*34*, *37*) differed from the current work in three ways. (1) The pH was 8.0 in the previous work and 7.0 in ours. (2) GST−N-WASP WWA or GST−WAVE (Scar1) WA was used in previous work, while we used WASp WA cleaved from GST. (3) Unchelated calcium ions were present in the previous work, while we included EGTA in our buffers. We therefore performed actin filament pelleting assays under all of these conditions using either WASp WA or Scar1 WA. Although the level of supernatant actin increases slightly with WASp or Scar1 WA, neither polypeptide causes actin depolymerization to the extent found in previous studies (Figure 4 and not shown). Densitometric analysis of the Coomassie-stained gels reveals that 4 μM WASp WA, whether coupled to GST or cleaved from it, increases the concentration of actin in the supernatant from 0.1 to 0.3 μM

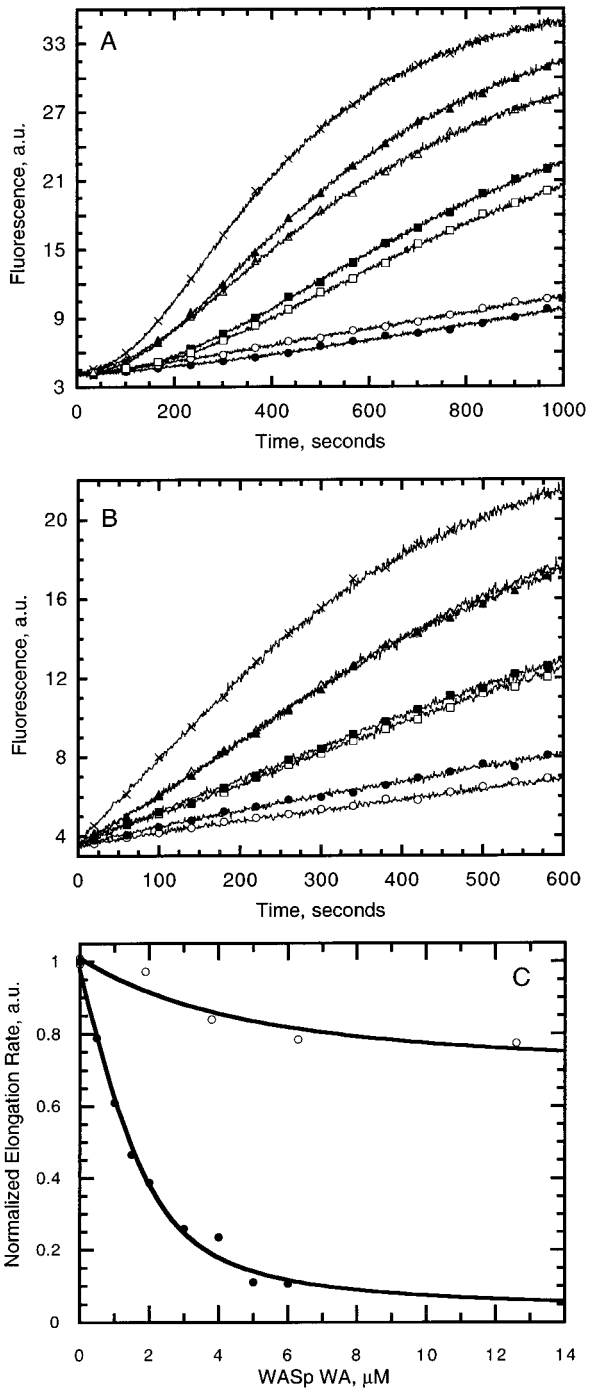

FIGURE 3: Effect of WASp WA and WH2 on actin polymerization. (A) WA and WH2 retard the polymerization of monomeric actin. To a final concentration of 4 μM monomeric Mg−actin (5% pyrene-labeled) was added 0 (×), 1 (▲), 2 (■), or 4 μM WA (●) or 10 (△), 20 (□), or 40 μM WH2 (○) in a final concentration of 1× polymerization buffer (pH 7.0), and the pyrene fluorescence was measured. (B) WA and WH2 inhibit pointed end elongation. Monomeric actin was incubated as described for panel B with varying amounts of WA or WH2. Then 60 μL of the same buffer, 20 μL of polymerization buffer, and 20 μL of 80 nM gelsolin−actin seeds were added, and the increase in pyrene fluorescence was measured. Symbols indicate the same final WA and WH2 concentrations as in panel A. (C) Dependence of the WA concentration on elongation rate from gelsolin-capped actin and spectrin−actin seeds. Actin monomers (2 μM, 5% pyrene-labeled) were added to 4 nM gelsolin−actin (●) seeds or to 0.4 nM spectrin−actin seeds (○) in the presence of varying amounts of WA. Elongation rates were measured for the initial 50 s and normalized to the rates in the absence of WA.

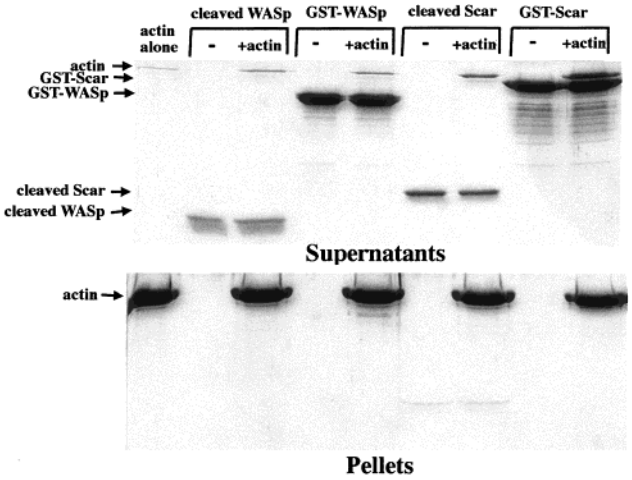

FIGURE 4: Neither WASp nor Scar1 WA depolymerizes actin filaments. Final concentrations of 4 μM polymerized actin and 4 μM WASp or Scar1 WA cleaved from GST, WASp, or Scar1 WA still attached to GST were incubated in 1× KMEI at pH 7.0 for 30 min at 25 °C. After centrifugation in a TLA-100 rotor at 80000*g* for 20 min, the pellets and supernatants were analyzed by SDS−PAGE and Coomassie staining. Similar results were obtained when Tris-HCl (pH 8.0) was used as the buffer or when EGTA was excluded from the buffer (not shown).

(4 μM total actin). Scar1 WA behaves in a similar manner when cleaved from GST, while GST−Scar1 increases the supernatant actin concentration to 0.7 μM.

Conditions for Nucleation by WA and the Arp2/3 Complex. WASp/Scar proteins act synergistically with the Arp2/3 complex to accelerate actin nucleation (*17*, *38*−*40*). To understand this process in more detail, we tested the effects of pH, nucleotide bound to actin monomers and filaments, and pyrene labeling of actin, as well as the concentration dependence of the Arp2/3 complex, WA actin monomers, and actin filaments. The Arp2/3 complex and WA affect two parameters of actin polymerization: the polymerization lag, during which stable nuclei form, and the concentration of filament ends that are generated, which is proportional to the polymerization rate at any given concentration of actin monomers. We analyze both parameters, expressing the polymerization lag as a nucleation rate (reciprocal of the time required for 10% polymerization) and calculating the concentration of ends generated from the polymerization rate at 80% of total polymerization. This method for calculating ends agrees well with elongation assays using the fully polymerized samples as seeds (not shown).

The pH affects the initial lag, which is much longer at pH 8.0 than at pH 6.5 in the presence and absence of WA and the Arp2/3 complex (Figure 5). With the Arp2/3 complex and WA, the nucleation rate is more than 5 times faster at pH 6.5 than at pH 8.0. However, when the effect of pH on elongation rate of actin alone is taken into account, the concentration of ends produced by WA and the Arp2/3 complex varies by less than a factor of 2 between pH 6.5 and 8.0. These effects are independent of the pH buffers that are used.

Nucleation by WA and the Arp2/3 complex is sensitive to the state of actin monomers in the assay. Pyrene−actin monomers are much less effective than unlabeled monomers in nucleating filaments in the presence of the Arp2/3 complex and WA, as judged by both the number of filaments produced

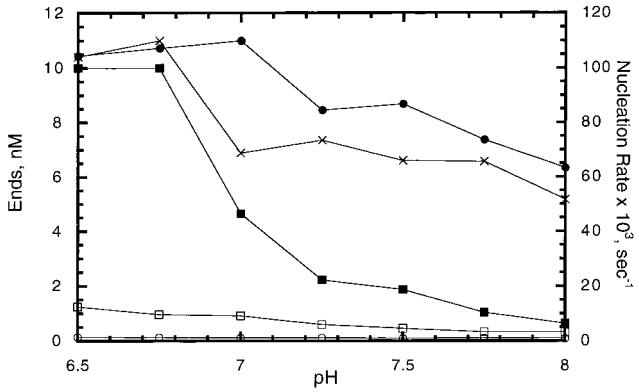

FIGURE 5: Effect of pH on actin polymerization in the absence and presence of WA and the Arp2/3 complex. The concentration of barbed ends (circles) and the nucleation rate (squares) as a function of pH in the absence (white symbols) and presence (black symbols) of WA and the Arp2/3 complex. The concentration of ends in the presence of WA, the Arp2/3 complex, and 250 nM phalloidin-stabilized polymerized actin was also determined (×).

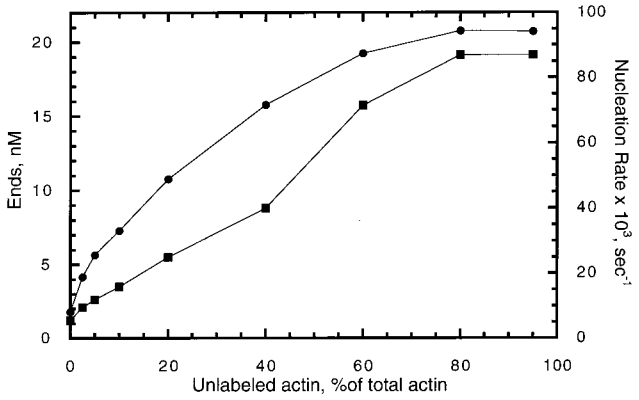

FIGURE 6: Effect of the percentage of pyrene−monomeric actin on WA or Arp2/3 stimulation. To a final concentration of 4 μM monomeric Mg−actin was added a final concentration of 1× KMEI without or with 500 nM WA and 50 nM Arp2/3 complex. The polymerization kinetics of different percentages of pyrene actin alone were indistinguishable from those of 100% pyrene−actin. The concentration of barbed ends (●) and the nucleation rate (■) are plotted as a function of the percentage of unlabeled monomeric actin.

and the polymerization lag (Figure 6). However, with less than 20% pyrene−actin, the effect of pyrene is minimal. Thus, our use of 5% pyrene−actin in other experiments does not affect the results. To test one possible reason for inhibition of WA and Arp2/3 complex-stimulated nucleation by pyrene−actin, we tested whether WA could inhibit elongation of 100% pyrene−actin from gelsolin−actin seeds. Approximately 2-fold more WA is required to inhibit pointed end elongation (not shown), so WA may bind less well to pyrene−actin monomers.

ATP−actin is a much better substrate than ADP−actin for nucleation by WA and the Arp2/3 complex, although high concentrations of the Arp2/3 complex and WA do enhance nucleation of ADP−actin (Figure 7). This effect is not due to a decreased affinity of WA for ADP-actin, as WA inhibits elongation of ADP−actin and ATP−actin monomers from gelsolin−actin seeds with a similar concentration dependence (not shown).

Concentration Dependence of Reactants during Nucleation. Nucleation depends on the concentrations of the Arp2/3 complex, WA, and MgATP−actin. With a constant

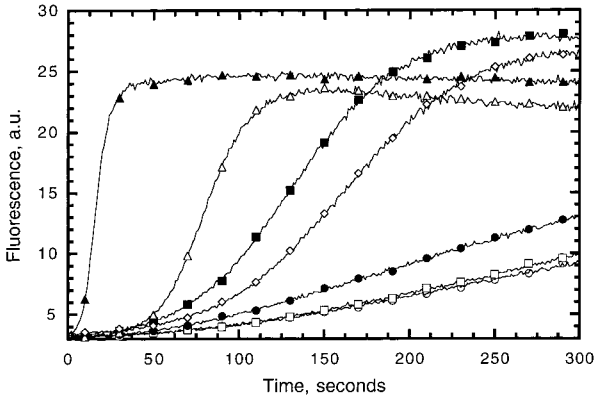

FIGURE 7: Monomeric MgATP−actin is a better substrate for nucleation by WA and the Arp2/3 complex than monomeric MgADP−actin. To a final concentration of 4 μM monomeric MgATP−actin (black symbols) or monomeric MgADP−actin (white symbols) were added no WA and the Arp2/3 complex (circles), 100 nM WCA and 10 nM Arp2/3 complex (squares), or 500 nM WA and 50 nM Arp2/3 complex (triangles) in a final concentration of 1× polymerization buffer (pH 7.0), and the pyrene fluorescence was measured. The white diamonds represent data for monomeric MgADP−actin which was preincubated with a 5-fold molar excess of ATP (0.5 mM) to free ADP in G-buffer for 3 min before starting polymerization in the presence of 100 nM WA and 10 nM Arp2/3 complex.

actin monomer concentration of 4 μM and an excess of WA, the nucleation rate and the number of filament ends produced increase with the concentration of the Arp2/3 complex (panels A and B of Figure 8). The nucleation rate reaches a maximum, and the concentration of filament ends plateaus at 20−25 nM with a saturating concentration of Arp2/3 complex. With <10 nM Arp2/3 complex and a saturating concentration of WA, each Arp2/3 complex produces one filament. Similarly, with constant concentrations of actin monomers and Arp2/3 complex, both parameters increase with WA concentration, and the concentration of ends again plateaus at 25 nM (Figure 8C).

With constant concentrations of the Arp2/3 complex and WA, both the concentration of ends and the nucleation rate increase with the concentration of monomeric actin (panels A and B of Figure 9). Both of these parameters also increase with actin concentration in the absence of the Arp2/3 complex or WA. The largest effect of WA and the Arp2/3 complex is at low actin concentrations. We found previously that the presence of profilin suppresses spontaneous nucleation and increases the contribution of activated Arp2/3-induced nucleation.

Effect of Preformed Filaments on Nucleation. Addition of polymerized actin greatly accelerates nucleation mediated by *Acanthamoeba* Arp2/3 complex and Scar constructs (*17*), so we investigated the effect of filaments on nucleation by the human Arp2/3 complex and WASp WA using two approaches. In the first approach, the presence of low concentrations of polymerized actin decreases the polymerization lag by the Arp2/3 complex and WA (Figure 10A). We used submaximal concentrations of WA and the Arp2/3 complex to slow the process so that the effect of filaments could be analyzed more accurately. While decreasing the lag, filaments have little effect on the number of new ends created by the Arp2/3 complex and WA. Although the vast majority of actin present in the filaments used in this experiment is in the ADP-bound state, the effect is similar when the

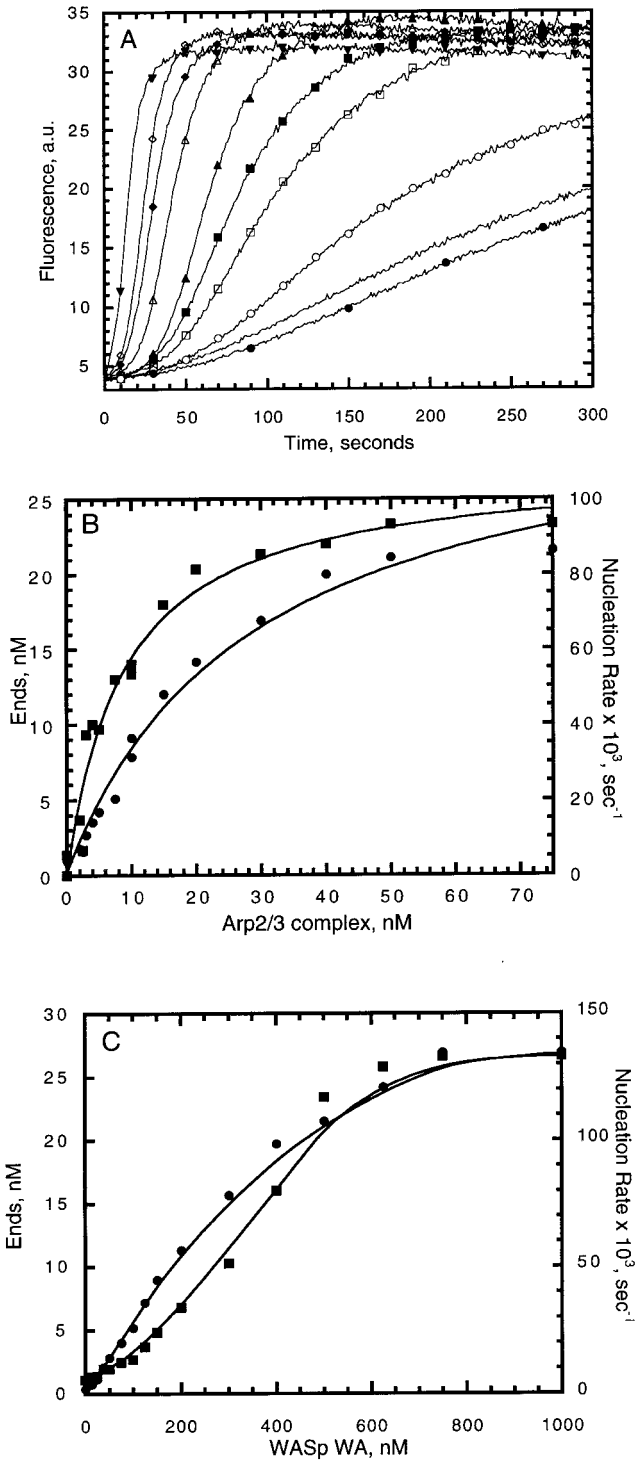

FIGURE 8: Nucleation depends on the concentrations of the Arp2/3 complex and WA. (A) Effect of the Arp2/3 complex concentration on actin polymerization in the presence of 4 μM monomeric actin and 0.5 μM WA. The Arp2/3 complex concentrations were 0 (●), 2 (○), 4 (□), 7.5 (■), 10 (▲), 15 (△), 20 (◆), 30 (◇), and 50 nM (▼). The trace with no symbols represents actin alone. (B) Calculation of the concentration of barbed ends (●) and nucleation rate (■) from data similar to those depicted in panel A. (C) Effect of WA concentration on the same parameters in the presence of 4 μM monomeric actin and 50 nM Arp2/3 complex.

filaments are in either the ADP−P_i- or ADP−BeF_3-bound state, or when the filaments are polymerized in the presence of excess phalloidin or when phalloidin is added after actin has fully polymerized (not shown). The pH dependence of nucleation by WA and the Arp2/3 complex appears to be

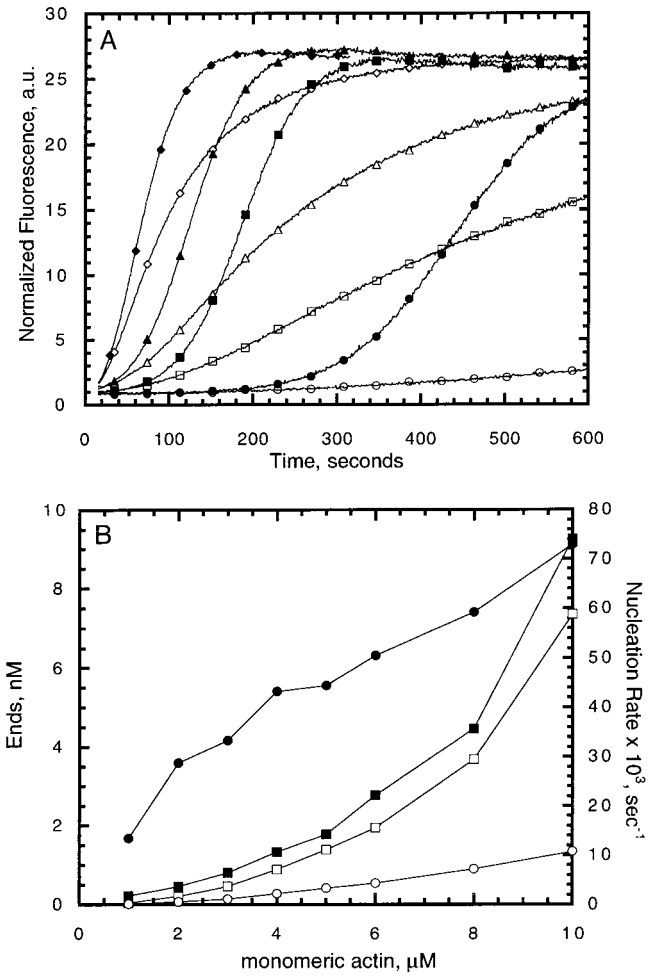

FIGURE 9: Effect of the monomeric actin concentration on nucleation by the Arp2/3 complex and WA. (A) Effect of the monomeric actin concentration on polymerization in the absence (white symbols) or presence (black symbols) of 100 nM WA and 10 nM Arp2/3 complex. The monomeric actin concentrations were 2 (circles), 4 (squares), 6 (triangles), and 10 μM (diamonds). (B) Calculation of concentration of barbed ends (circles) and nucleation rate (squares) in the absence (white symbols) or presence (black symbols) of 100 nM WA and 10 nM Arp2/3 complex from polymerization data similar to those depicted in panel A.

similar in the presence and absence of filaments, as the number of ends created by WA and the Arp2/3 complex in the presence of filaments is also affected by less than a factor of 2 between pH 6.5 and 8.0 (Figure 5B).

As another test for filament stimulation of nucleation by WA and the Arp2/3 complex, we initiated the spontaneous polymerization of actin monomers alone, and then added the Arp2/3 complex and WA at various times during the reaction. The lag for nucleation by the Arp2/3 complex and WA declines progressively during spontaneous polymerization of actin alone (Figure 10B), suggesting that the actin polymerized spontaneously stimulates nucleation by WA and the Arp2/3 complex. The concentrations of polymerized actin needed to increase the nucleation rate by the Arp2/3 complex and WA are similar in the two types of experiments (Figure 10C).

DISCUSSION

Effect of WASp WA Alone on Actin Dynamics. Our study is the first quantitative analysis of the interaction between WASp/Scar proteins and actin. In the pointed end elongation assay, WASp WA binds actin monomers with an apparent K_d of 0.4 μM. This interaction inhibits addition of monomers to filament pointed ends but not to barbed ends, since excess WA inhibits only slightly elongation from prepolymerized actin seeds. Since WA also inhibits spontaneous polymerization of actin from monomers, and pointed end elongation contributes little to this process, WA must also inhibit spontaneous nucleation. The WH2 motif alone affects actin polymerization similarly but with a 10-fold lower affinity. Finally, in contrast to the work of others (*32*−*34*), we find that neither WASp WA nor Scar1 WA depolymerizes preformed actin filaments to the same extent. The level of depolymerization is negligible with WASp WA, Scar WA, or GST−WASp WA, while GST−Scar1 WA depolymerized <20% of 4 μM actin, much less than that observed by others (*34*). We see no simple explanation for this discrepancy, but it may be related to the method of actin preparation, which was not described in the previous work.

Inhibition of pointed end elongation by WA and WH2 implies that they may bind to domain 1 and/or domain 3 of actin monomers (*41*), sterically inhibiting addition of these complexes at pointed ends but not at barbed ends (Figure 11A). Since WA only slightly inhibits barbed end elongation at the concentrations we tested, it must rapidly dissociate from the filament barbed end upon addition of WA-bound monomer. Profilin has a similar effect on polymerization; it inhibits nucleation and pointed end elongation but not barbed end elongation (*35*). This is due to binding to actin subdomains 1 and 3 (*42*−*44*). On the other hand, WA differs from profilin in that it does not catalyze nucleotide exchange on actin. WASp/Scar WH2 has some sequence motifs similar to those of the sequestering protein thymosin β4 (Tβ4) in the region that binds actin subdomains 1 and 3. WH2 contains a sequence similar to the KLKK motif of Tβ4, in which the second lysine can be cross-linked to an acidic residue in subdomain 1 of actin (*45*). Another similarity to Tβ4 is the high level of conservation of several hydrophobic residues in the 10 amino acids directly N-terminal to the KLKK motif. In Tβ4, modifications of analogous residues reduce the affinity for actin (*46*, *47*). Last, WASp/Scar WH2 motifs contain a highly conserved basic residue 12 amino acids N-terminal to the KLKK-like motif. A lysine in a similar position on Tβ4 cross-links an aspartate on subdomain 3 of actin (*45*). The 10-fold lower affinity of WH2 than of WA for actin suggests that residues C-terminal to the WH2 might also contribute to actin binding.

Nucleation by the Arp2/3 Complex and WA. This study is an initial step in dissecting the details of nucleation by the Arp2/3 complex and WA. By analyzing two parameters of the process, the nucleation rate and the number of ends produced, we can judge the effect of changing conditions on the nucleation process. The nucleation rate reflects the ensemble of the associations required for formation of a nucleus. These associations could include actin monomers to form dimers or trimers, WA with an actin monomer, WA with the Arp2/3 complex, WA−actin with the Arp2/3 complex, the WA−actin monomer−Arp2/3 complex with additional actin monomer(s), and the Arp2/3 complex with the side of an actin filament. Similarly, dissociation rates of these complexes will affect nucleation. The potential of each of these associations to affect the others lends a high level

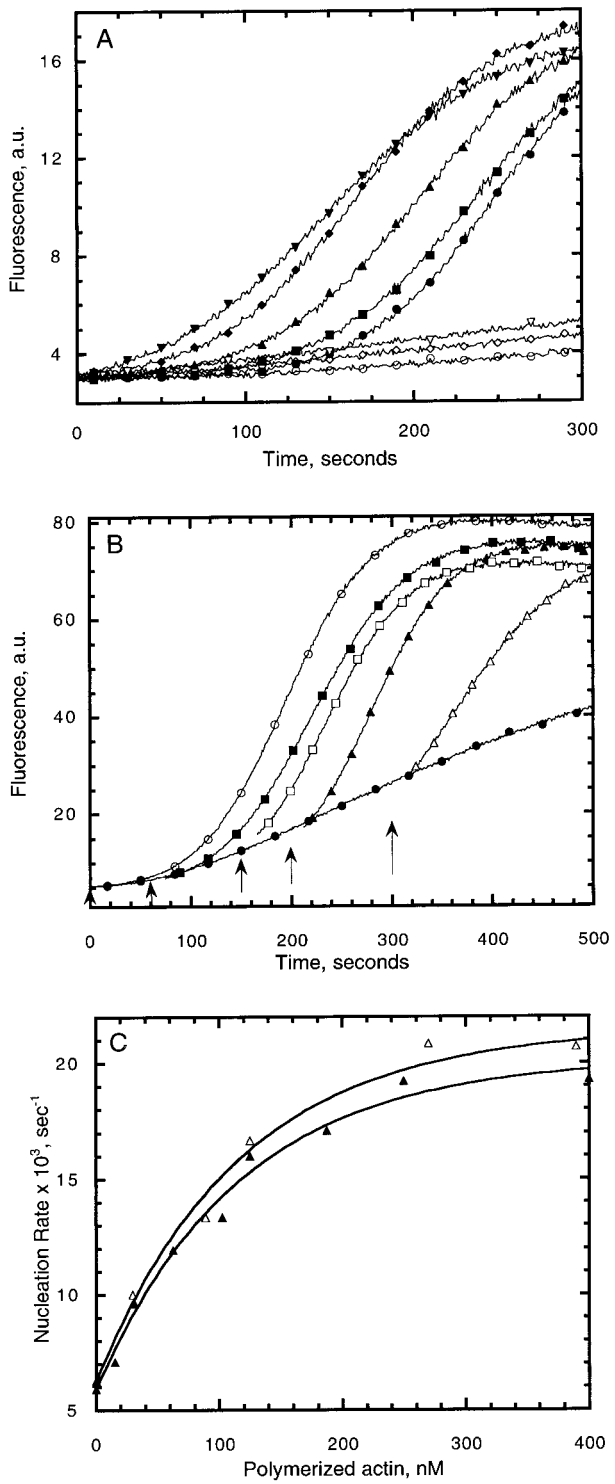

FIGURE 10: Prepolymerized actin enhances WA and Arp2/3 complex stimulation of actin polymerization. (A) Effect of prepolymerized actin addition to 2 μM monomeric actin in 1× KMEI in the absence (white symbols) or presence (black symbols) of 2 μM monomeric actin, 100 nM WA, and 10 nM Arp2/3 complex. The prepolymerized actin concentrations were 0 (circles), 16 (squares), 32 (triangles), 100 (diamonds), and 250 nM (inverted triangles). (B) Effect of delayed addition of 100 nM WA and 10 nM Arp2/3 complex to 2 μM monomeric actin under polymerizing conditions. WA and Arp2/3 complex were added at 0 (○), 60 (■), 150 (□), 200 (▲) or 300 s (△) after initiation of polymerization. The data for no addition of WA and Arp2/3 complex are depicted as black circles. (C) Relationship between the concentration of added polymerized actin depicted in panel A (▲) or the concentration of actin that had formed before addition of WA and the Arp2/3 complex depicted in panel B (△) and the nucleation rate.

of potential complexity. The number of ends produced represents the total efficiency of the process. We assume that by obtaining a 1:1 correspondence between ends produced and Arp2/3 complex at low Arp2/3 complex concentrations we have reached 100% efficiency, although this might not be the case. A full understanding of the nucleation process will require measurement of affinities and rates of each association and their effects on other associations.

Concentration Dependence of the Arp2/3 Complex for Nucleation. The Arp2/3 complex activated by excess WASp WA saturates in nucleation reactions at <50 nM, or >100-fold lower than its cellular concentration of 9.7 μM in neutrophils. This is also true when excess Scar1 WA activates the Arp2/3 complex (not shown). The reason excess Arp2/3 complex does not nucleate more filaments is not clear. One possibility is that activation of the Arp2/3 complex is slow, so explosive polymerization at saturating Arp2/3 complex concentrations depletes actin monomers before most of the Arp2/3 complex is active. This depletion would be independent of the actin monomer concentration, since the rate of monomer addition to the barbed end is proportional to monomer concentration (10 μM monomer^{-1} s^{-1}). Cellular Arp2/3 complex activation would not be subject to the same limitation, since the pool of unpolymerized actin monomers bound to profilin or Tβ4 is constantly replenished by filament turnover (*48*). Rapid capping of new barbed ends might also limit the depletion of the subunit pool in the cell (*49*).

Role of Filament Side Binding in Nucleation by the Arp2/3 Complex. We previously showed that addition of actin filaments reduces the nucleation lag by the *Acanthamoeba* Arp2/3 complex and human Scar1 WA (*17*). This finding supports the dendritic nucleation model, and suggests that filament side binding and filament nucleation by the Arp2/3 complex might be tightly linked. In this study, we examine this effect in more detail in an effort to determine whether preformed filaments are necessary for Arp2/3 complex-mediated nucleation, or if they stimulate but are not required. Our evidence suggests the latter. Saturating concentrations of WA and the Arp2/3 complex practically eliminate the lag. WA slows nucleation in the absence of the Arp2/3 complex, so nucleation with saturating WA and the Arp2/3 complex appears to occur in the absence of filaments. However, preformed filaments clearly stimulate nucleation by the Arp2/3 complex and WA. Addition of preformed filaments reduces the nucleation lag in a saturatable manner. In addition, the nucleation lag is progressively reduced when actin is allowed to polymerize for varying times before addition of the Arp2/3 complex and WA, and the filament concentration dependence of this effect is similar to that of added filaments. The results of varying pH and monomeric actin concentration are also suggestive of a stimulatory effect by filaments, as in both cases increasing the rate of spontaneous polymerization increases the rate of nucleation by the Arp2/3 complex and WA. Filaments might therefore make WA binding to the Arp2/3 complex more favorable, especially in cells where the concentration of filaments is about 2 orders of magnitude higher than in our experiments.

The cellular importance of the filament effect will likely depend on the concentrations of the Arp2/3 complex, WASp/Scar proteins, and polymerized actin at areas of actin polymerization. The concentration of the Arp2/3 complex

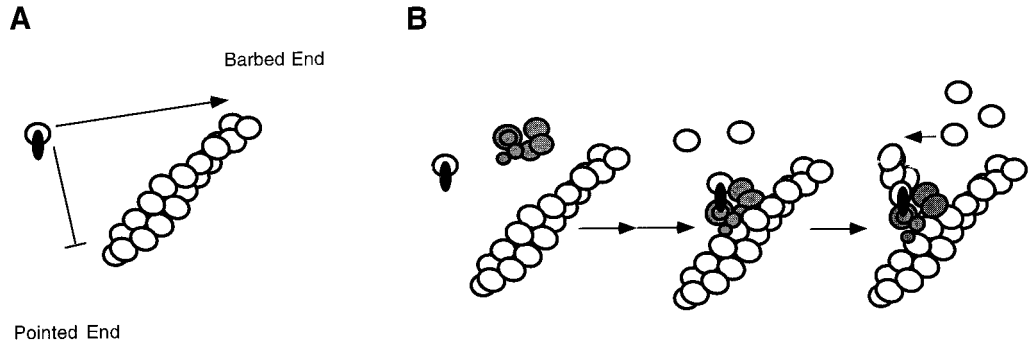

FIGURE 11: Models for the WASp WA effect on actin and the Arp2/3 complex. (A) WASp WA (black oval) binds to actin monomers (white circle), preventing their addition to pointed ends, but not barbed ends, of actin filaments. (B) The Arp2/3 complex (gray circles) binds actin filaments and WASp WA bound to an actin monomer in an undefined order. The actin monomer bound to WASp WA serves to complete the nucleus on the activated Arp2/3 complex, allowing elongation.

in neutrophils (9.7 μM) is supersaturating for nucleation according to our assays. The cellular concentrations of WASp/Scar proteins are unknown, but may be much lower than those of the Arp2/3 complex. Furthermore, the cellular concentrations of WASp/Scar proteins capable of activating the Arp2/3 complex are probably lower than the total WASp/Scar concentration, since activation of WASp/Scar proteins by Cdc42, PIP_2, or other factors is presumably required to activate the Arp2/3 complex in turn (*13*). Another factor is the localized concentration of the Arp2/3 complex and WASp/Scar proteins, which would also affect activation. The high concentration of polymerized actin at the leading edge means that this activator of Arp2/3 complex-mediated nucleation is not limiting and could serve to drive the process.

Nucleation Mechanism of the Arp2/3 Complex and WA. A preliminary model for nucleation by the Arp2/3 complex and WA is shown in Figure 11B. The region of WASp/Scar proteins involved in activating nucleation by the Arp2/3 complex includes the actin monomer binding WH2 motif and the Arp2/3 complex binding acidic motif. The mechanism of activation is far from understood, but it is worth considering two types of mechanisms, which may be complementary. WASp/Scar proteins may activate nucleation by the Arp2/3 complex by altering its conformation, possibly by allowing Arp2 and Arp3 to mimic a barbed end (*5*). In addition, WASp/Scar proteins may position an actin monomer on this dimer to "jump start" the process. Polymerized actin may augment nucleation by promoting either process or both processes. For example, Arp2/3 complex binding to the side of a filament might stabilize interactions of the complex with WA. Knowledge of the affinity of the multiple partners in this process for each other will be required to sort out the mechanism. Other potential effects of the Arp2/3 complex and WA, such as on filament annealing or on polymerization rate constants, will also have to be evaluated.

Purification of the Arp2/3 Complex from Human Leukocytes. Although several purification schemes for the mammalian Arp2/3 complex exist (*7*, *9*, *30*), we developed a faster procedure for minimizing artifacts due to the possible instability of the complex. This rapid purification may be the reason that our Arp2/3 complex has a higher specific activity than other preparations. With <10 nM Arp2/3 complex in the presence of a saturating concentration of WA, there is a 1:1 correspondence between the Arp2/3 complex and filaments produced, and at a saturating concentration of the Arp2/3 complex, it nucleates 20−25 nM filaments. This ratio is significantly better than those we calcluated from other published results: 8 nM filaments created from 60 nM Arp2/3 complex (1 filament per 30 Arp2/3 complexes; *38*) and 8 nM filaments created from 20 nM Arp2/3 complex (1 filament per 10 Arp2/3 complexes; *40*). Fully active Arp2/3 complex is essential to our goal of understanding the mechanism of nucleation.

ACKNOWLEDGMENT

We thank members of the Pollard lab for technical assistance, advice, and helpful discussion. We thank Jill Meisenhelder for synthesis of the WH2 peptide.

REFERENCES

1. Mitchison, T. J., and Cramer, L. P. (1996) *Cell 84*, 371−379.
2. Carson, M., Weber, A., and Zigmond, S. H. (1986) *J. Cell Biol. 103*, 2707−2714.
3. Chan, A. Y., Raft, S., Bailly, M., Wyckoff, J. B., Segall, J. E., and Condeelis, J. S. (1998) *J. Cell Sci. 111*, 199−211.
4. Pollard, T. D., and Cooper, J. A. (1986) *Annu. Rev. Biochem. 55*, 987−1035.
5. Mullins, R. D., and Pollard, T. D. (1999) *Curr. Opin. Struct. Biol. 9*, 244−249.
6. Kelleher, J. F., Atkinson, S. J., and Pollard, T. D. (1995) *J. Cell Biol. 131*, 385−397.
7. Machesky, L. M., Reeves, E., Wientjes, F., Mattheyse, F. J., Grogan, A., Totty, N. F., Burlingame, A. L., Hsuan, J. J., and Segal, A. W. (1997) *Biochem. J. 328*, 105−112.
8. Welch, M. D., DePace, A. H., Verma, S., Iwamatsu, A., and Mitchison, T. J. (1997) *J. Cell Biol. 138*, 375−384.
9. Ma, L., Rohatgi, R., and Kirschner, M. W. (1998) *Proc. Natl. Acad. Sci. U.S.A. 95*, 15362−15367.
10. Mullins, R. D., and Pollard, T. D. (1999) *Curr. Biol. 9*, 405−415.
11. Mullins, R. D., Heuser, J. A., and Pollard, T. D. (1998) *Proc. Natl. Acad. Sci. U.S.A. 95*, 6181−6186.
12. Welch, M. D., Rosenblatt, J., Skoble, J., Portnoy, D. A., and Mitchison, T. J. (1998) *Science 281*, 105−108.
13. Higgs, H. N., and Pollard, T. D. (1999) *J. Biol. Chem. 274*, 32531−32534.
14. Svitkina, T. M., Verkhovsky, A. B., McQuade, K. M., and Borisy, G. G. (1997) *J. Cell Biol. 139*, 397−415.
15. Svitkina, T. M., and Borisy, G. G. (1999) *J. Cell Biol. 145*, 1009−1026.
16. Bailly, M., Macaluso, F., Cammer, M., Chan, A., Segall, J. E., and Condeelis, J. S. (1999) *J. Cell Biol. 145*, 331−345.
17. Machesky, L. M., Mullins, D. M., Higgs, H. N., Kaiser, D. A., Blanchoin, L., May, R. C., Hall, M. E., and Pollard, T. D. (1999) *Proc. Natl. Acad. Sci. U.S.A. 96*, 3739−3744.
18. Machesky, L. M., and Insall, R. H. (1998) *Curr. Biol. 8*, 1347−1356.

19. Schmid-Schonbein, G. W., Shih, Y. Y., and Chien, S. (1980) *Blood 56*, 866−875.
20. Spudich, J. A., and Watt, S. (1971) *J. Biol. Chem. 246*, 4866−4871.
21. Pollard, T. D. (1984) *J. Cell Biol. 99*, 769−777.
22. Houk, T. W., Jr., and Ue, K. (1974) *Anal. Biochem. 62*, 66−74.
23. Cooper, J. A., Walker, S. B., and Pollard, T. D. (1983) *J. Muscle Res. Cell Motil. 4*, 253−262.
24. Pollard, T. D. (1986) *J. Cell Biol. 103*, 2747−2754.
25. Carlier, M.-F., and Pantaloni, D. (1988) *J. Biol. Chem. 263*, 817−825.
26. Combeau, C., and Carlier, M.-F. (1988) *J. Biol. Chem. 263*, 17429−17436.
27. Bryan, J. (1988) *J. Cell Biol. 106*, 1553−1562.
28. Casella, J. F., Maack, D. J., and Lin, S. (1986) *J. Biol. Chem. 261*, 10915−10921.
29. Pollard, T. D. (1984) *J. Cell Biol. 99*, 1970−1980.
30. Welch, M. D., Iwamatsu, A., and Mitchison, T. J. (1997) *Nature 385*, 265−269.
31. Kelleher, J. F., Mullins, R. D., and Pollard, T. D. (1998) *Methods Enzymol. 298*, 42−51.
32. Miki, H., Miura, K., and Takenawa, T. (1996) *EMBO J. 15*, 5326−5335.
33. Miki, H., and Takenawa, T. (1998) *Biochem. Biophys. Res. Commun. 243*, 73−78.
34. Miki, H., Suetsugu, S., and Takenawa, T. (1998) *EMBO J. 17*, 6932−6941.
35. Pollard, T. D., and Cooper, J. A. (1984) *Biochemistry 23*, 6631−6641.
36. Pring, M., Weber, A., and Bubb, M. (1992) *Biochemistry 31*, 1827−1836.
37. Miki, H., Sasaki, T., Takai, Y., and Takenawa, T. (1998) *Nature 391*, 93−96.
38. Rohatgi, R., Ma, L., Miki, H., Lopez, M., Kirchhausen, T., Takenawa, T., and Kirschner, M. W. (1999) *Cell 97*, 221−231.
39. Winter, D., Lechler, T., and Li, R. (1999) *Curr. Biol. 9*, 501−504.
40. Yarar, D., To, W., Abo, A., and Welch, M. D. (1999) *Curr. Biol. 9*, 555−558.
41. Kabsch, W., Mannherz, H. G., Suck, D., Pai, E., and Holmes, K. C. (1990) *Nature 347*, 37−44.
42. Vandekerckhove, J., Kaiser, D. A., and Pollard, T. D. (1989) *J. Cell Biol. 109*, 619−626.
43. Schutt, C., Myslik, J. C., Rozychi, M. D., Goonesekere, N. C. W., and Lindberg, U. (1993) *Nature 365*, 810−816.
44. Kaiser, D. A., and Pollard, T. D. (1996) *J. Mol. Biol. 255*, 89−107.
45. Safer, D., Sosnick, T. R., and Elzinga, M. (1997) *Biochemistry 36*, 5806−5816.
46. Van Troy, M., Dewitte, D., Goethals, M., Carlier, M. F., Vanderkerckhove, J., and Ampe, C. (1996) *EMBO J. 15*, 201−210.
47. Heintz, D., Reichert, A., Mihelicr., M., Stoeva, S., Voelter, W., and Faulstich, H. (1994) *Eur. J. Biochem. 223*, 345−350.
48. Theriot, J. A., and Mitchison, T. J. (1991) *Nature 352*, 126−131.
49. Schafer, D. A., Jennings, P. B., and Cooper, J. A. (1996) *J. Cell Biol. 135*, 169−179.

BI991843+